

Effect of intake manifold water injection on a natural gas spark ignition engine: an experimental study

H Arruga¹, F Scholl¹, M Kettner^{1*}, O I Amad², M Klaissle³, B Giménez⁴

¹ Karlsruhe University of Applied Sciences, Germany

² Universiti Malaysia Pahang

³ SenerTec Kraft-Wärme-Energiesysteme GmbH, Germany

⁴ University of Valladolid, Spain

*Corresponding author: maurice.kettner@hs-karlsruhe.de

Abstract. Design and development of gas CHP (combined heat and power) engines are strongly influenced by the progressively more severe European NO_x emissions normative. Water injection represents a promising approach to reduce these emissions while attaining high engine efficiency. In this work, the effect of intake manifold water injection on combustion parameters and performance of a single-cylinder naturally aspirated natural gas spark ignition engine is presented. First, the most appropriate injector was selected, using a spray test bed. Subsequently, engine experiments at constant indicated mean effective pressure (IMEP) and engine speed were conducted with water-fuel ratios of 0.1 to 0.3. IMEP was kept constant at about 6.3 bar by adjusting both air-fuel ratio and spark timing. A NO_x reduction of 0.2 g/kWh_i (15 %) for a constant ISFC of about 204 g/kWh_i was achieved. In the low NO_x regime, water injection allows for an improvement of the NO_x-ISFC trade-off, while leading to poor fuel consumption at same NO_x in the high efficiency regime. Furthermore, water injection implies a reduction of intake mixture temperature, lengthened burning delay and combustion duration and a moderate increase of combustion instability.

1. Introduction

Combined heat and power systems have gained increasing relevance in the last years in the field of decentralised energy supply. By recovering waste heat while generating electric power, a high overall efficiency of the unit is achieved. Natural gas CHP units often operate with lean air-fuel mixtures ($\lambda > 1$) in order to meet the NO_x emissions limits imposed by legislation at high engine efficiency. These operating conditions further reduce the knocking tendency of the engine, allowing for high compression ratios. The reduction of HC and CO emissions is less problematic than that of NO_x, as oxidation catalysts still function under excess of oxygen and can be used for after treatment as long as exhaust gas temperature are above a certain level. Figure 1a shows the NO_x emissions of a gas engine as a function of λ (relative air-fuel ratio) qualitatively. As it can be seen, there is a limit determined by engine knock and a lean-burn limit due to misfires.



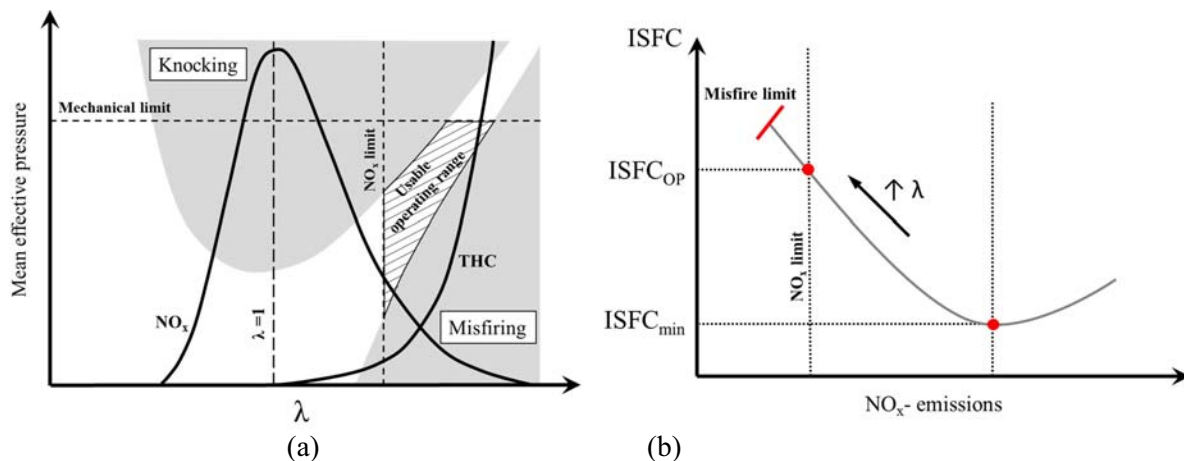


Figure 1. Lean-burn combustion: Mean effective pressure operating map of a gas engine as a function of relative air-fuel ratio [9] (a), NO_x-ISFC trade-off for gas engines (b).

As λ is increased in order to reduce NO_x emissions, combustion temperature and flame speed decrease and combustion instability increases. The combustion then diverges from the optimal isochoric combustion at TDC, which is reflected in a worsened ISFC (and a decrease of indicated efficiency). This is shown in the NO_x-ISFC trade-off diagram in figure 1b. The engine works in an operating point with higher ISFC but with a NO_x emissions level that fulfils the normative.

In Germany, the emissions of gas engines with a fuel input power above 1 MW are regulated according to TA-Luft standards, which set the limits for NO_x emissions to 500 mg/Nm³. Smaller gas engines, typical for micro-CHP units, however, are currently not subject to specific emission requirements. In 2018, a new European norm will be introduced. It restricts NO_x to 240 mg/kWh fuel input in terms of GCV [6]. This implies that new measures need to be found to meet this stringent emission requirement without losses in engine efficiency and power.

Among the internal measures to reduce NO_x emissions and knock in spark ignition engines as, for example, exhaust gas recirculation (EGR), water injection offers a high potential. The main advantage lies in the higher heat capacity of water compared to N₂, O₂ and CO₂ (remaining main components of exhaust gas), as it is illustrated in figure 2a.

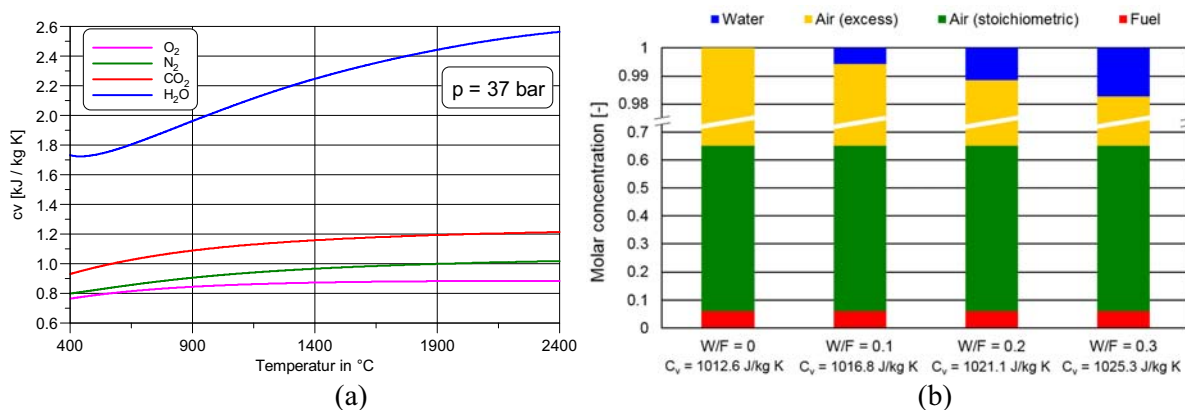


Figure 2. Constant volume heat capacity of several gases for $p = 37$ bar as a function of temperature (calculated with EES v.10) (a) and variation of the heat capacity of the mixture with water addition (b)

Figure 2b shows the variation in constant volume heat capacity of the mixture for $p = 37$ bar and $T = 890$ °C when water is added to the mixture, supposing that the amount of fuel does not vary. This pressure and temperature levels match approximately with the conditions at the end of compression stroke for the engine configuration used for water injection in this study. As it can be seen, water

replaces a part of the excess air and, due to the higher capacity of water respect to air, the total capacity of the mixture increases. The injected water is normally quantified using the variable water-fuel ratio (W/F). It is defined as the ratio between the mass flows of water and fuel in a particular operating point:

$$W / F = \frac{m_{fuel}}{m_{water, inj}} \quad (1)$$

According to equation (2), the increase of the heat capacity of the mixture leads to a lower temperature rise during combustion:

$$Q = m \cdot c_v \cdot \Delta T \quad (2)$$

with $Q = \text{const.}$, $m = \text{const.}$, $c_v \uparrow \Rightarrow \Delta T \downarrow$

Q is the heat release in J

m is the mass of in-cylinder charge in kg

c_v is the specific heat capacity of the in-cylinder charge in J/(kg · K)

ΔT is the increase in temperature due to combustion

In internal combustion engines, NO is usually present in higher concentration in exhaust gas compared to NO₂. Besides, the “thermal” NO formation has a dominant role over other mechanisms of NO formation. This reaction takes place for temperature values over approximately 1800 K and is accelerated exponentially with the increasing temperature [15]. Therefore, when the combustion temperature levels are lower due to the increase of the heat capacity, less NO_x is formed.

Another positive effect of water injection is the active cooling of the aspirated charge due to the endothermal process of evaporating the water in the intake manifold. Because of the lowered intake temperature, mixture temperature at the end of compression is also reduced. This reduces the knock tendency of the engine in middle and high-load operating points, thus allowing for an increase of the compression ratio with an increment of the efficiency and a fuel reduction [5][11][20]. The mixture temperature reduction arising from the evaporation enthalpy of water can be deduced from the following equation:

$$m_w \cdot \Delta h_{ev} = m_{charge} \cdot c_p \cdot \Delta T_{charge} \quad (3)$$

where m_w is the mass of injected water in kg/s

Δh_{ev} is the enthalpy of water evaporation in J/kg

m_{charge} is the mass of intake air in kg/s

c_p is the specific heat capacity in J/(kg · K)

ΔT_{charge} is the reduction of charge air temperature in K

The higher viscosity and the higher surface tension of water to petrol imply a worse atomization and breakup of the water spray. Furthermore, the lower vapour pressure of water compared to petrol causes worse evaporation of water droplets in the cylinder charge [11]. These factors need to be accounted for by choosing an optimal injector design and optimal injection parameters. The pre-warming of water before the injector could favour its evaporation by flash boiling of the droplets. It could be combined, for example, with exhaust gas heat recovery, using the energy of exhaust gas to heat up the water. The possibility of injecting water steam, as it was made by Kökkülünk et al. [14], is another strategy. However, the effect of charge cooling would be lost.

Water injection was introduced in 2015 by BMW in their M4 GTS model. Water is injected after the intercooler before the intake manifold of the turbocharged engine, using a water injector

specifically designed for this purpose [4]. The water is taken from a tank that needs to be refilled periodically [2]. The second generation of water injection was investigated by BMW combining water injection downstream the throttle valve and high-pressure direct injection of a mixture of petrol and water by means of a specially designed injector [3]. In this case, condensed water from the air conditioning system of the vehicle was used. As a result, an increase of the compression ratio and a reduction of 23 % in fuel consumption in g/kWh were achieved. Additionally, with water injection, operating with stoichiometric amount of fuel is also allowed in operation points where normally fuel enrichment is necessary. Therefore, the three-way catalyst is operating even at high engine load.

Water injection has been investigated in several gas engine research works. Subramanian et al. [19] used intake manifold water injection in a naturally aspirated single cylinder hydrogen-fuelled engine. In this case, water injection reduced NO emissions by 32 % with no loss in brake thermal efficiency (BTE). Pucher et al. [17] investigated the influence of intake manifold water injection in a town gas driven internal combustion engine. The water was brought in after the throttle valve using the carburettor injection principle. This setup enabled a maximal decrement of 60 % in NO_x emissions without a loss in engine power. More recently, Tschalamoff et al. [21] investigated the influence of direct water injection for a turbocharged 13.6 litre natural gas cogeneration engine. The influence of water injection on NO_x reduction, engine efficiency, knocking and possible increase of mean effective pressure was reported. With a water-fuel ratio of approximately 20 %, it was possible to reduce engine-out NO_x by 50 %. At the same time, however, an increment of HC and CO emissions together with losses in engine efficiency due to the slower combustion and lower combustion temperature was observed. Furthermore, the authors determined the optimal injection timing as well as the shift of the knock limit for different W/F ratios. Water injection during intake stroke showed the higher reduction of NO_x emissions. Under the effect of water injection, the knock limit moved towards earlier ignition timings. Tschalamoff et al. [22] also conducted experiments on intake manifold water injection on a natural gas 4.8 litre research engine. They found that intake manifold water injection has a stronger effect on NO_x decrease compared with direct water injection. Analogously, a higher burning delay and a slower combustion was observed, together with higher HC and CO emissions and reduced engine efficiency.

In this paper, the influence of intake manifold water injection on a small naturally aspirated spark ignition engine fuelled with natural gas will be studied. The experiments were carried out in the framework of a research project where the aim is to recirculate condensate from the exhaust gas. The objective of this work was to determine the feasibility of the developed water injection system and study the effect of increasing water injection ratios on emissions, combustion stability and engine efficiency.

2. Experimental equipment

2.1. Spray test bed

A spray test bed was built up to analyse and simulate water injection into the intake manifold of the gas engine, as shown in figure 3a. To this end, the cross section of the test bed channel was adjusted geometrically to that of the intake manifold. The duct consists of a square geometry confined by four slabs made of acrylic glass.

An adjustable aluminium profile is placed in the middle of the duct. Its bottom is heated by two contact heaters (type Omega KH-103/10-P and KH-104/10-P) with a heating power of 1.55 W/cm². The total surface of the heaters is 45 cm² and, therefore, the maximum provided power by the heaters is around 70 W. Their function is to vary the temperature of the middle profile to simulate different conditions of intake manifold wall temperature. Temperature is controlled by an Omega CN7823 PID controller from the reading of a self-adhesive thermocouple. The PWM (pulse width modulation) output of the controller is connected to a solid-state relay, which powers the heaters intermittently. The PWM duty cycle is closed-loop controlled to maintain the rated temperature constant.

A pivoting structure was designed to test different injection angles and study their influence on wall wetting. Water is fed to the injector from a tank, pressurised with compressed air. The water is

led to the injector using flexible polyethylene tubes and a special adapter for the injector. Tank pressure is controlled using a Festo LRP-1/4-10 high-precision pressure control valve.

An air conditioning unit provides the air mass flow through the test bed. It consists of a motor-driven compressor in series with a heat exchanger that allows adjusting both mass flow and air temperature at which injection testing is carried out. A Bosch HFM5-4.7 hot film air flow meter measures the intake air mass flow.

Spray images were captured employing a monochromatic CCD camera with a resolution of 9 megapixels and a maximum frame rate of 7 fps (figure 3b). The instant at which the image will be taken can be determined by either internal (software) or external triggers. The camera is fixed on a special mount, allowing for an adjustment of its horizontal and vertical position, as well as its distance to the spray test bed.

An infrared light source (Büchner HI-LIGHT-120) was used to light the water sprays evenly. This type of light source was selected because it provides higher contrast images. Moreover, the infrared light has a lower surface reflection as visible light on acryl glass and the water droplets can be better captured. An infrared filter was additionally coupled to the objective to reduce the distortion caused by other wavelengths from ambient light.

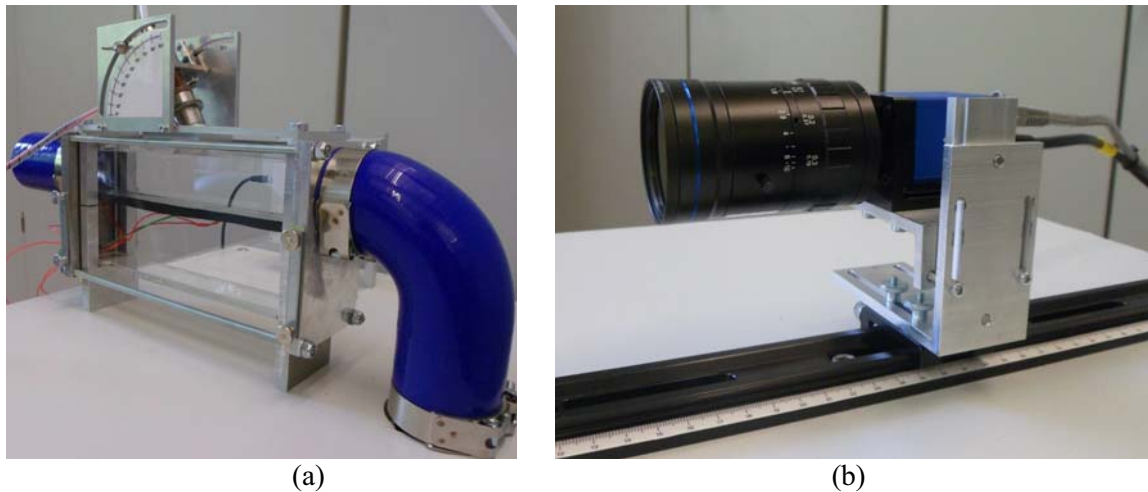


Figure 3. Spray test bed used for the injector tests and simulation of the intake manifold flow conditions (a), CCD-Camera SVS-Vistek eco815MTLGEC and Myutron HF5018V-2 objective used for taking the spray images (b).

An ADwin Gold-II control unit and LabVIEW software were employed for data acquisition and for triggering both the injector and the camera. Software SVCapture of the company SVS-Vistek was used to adjust the camera settings.

Three different petrol injectors were tested with water: one port fuel injector (PFI) and two gasoline direct injectors (GDI). All of them will be used with low injection pressure. Their main characteristics are summarised in table 1.

Table 1. Main characteristics of the tested (gasoline) injectors.

	Siemens 98MF-9F593-EXP10	Denso E7T05072	Bosch 0261500020
Injector type	Multi-hole injector	Swirl injector	Swirl injector
Injection type	PFI	GDI	GDI
Rated injection pressure	< 4 bar	≈ 80 bar	≈ 120 bar
Number of holes	2	1	1
Spray type	Full cone	Hollow cone	Hollow cone
Spray angle (α)	≈ 20°	≈ 57°	≈ 65°
Inclination angle (β) spray / injector axis	0°	0°	10°

Although swirl injectors are designed for high pressure, they provide relative small droplet sizes even at low injection pressures [1]. The hollow cone of the spray is due to the tangentially rotating flow inducted by the tangential fluid inlets inside the injector's swirl chamber. The Denso swirl injector was previously used by Kettner et al. [12] for injecting water at the intake port of a diesel engine.

While injectors with lower spray angle cause less wall wetting, the spray covers less volume of the air mass flow and an even dispersion of the injected water becomes more challenging. Therefore, a compromise between these two characteristics must be found. In addition, the injector must provide an adequate quantity of water according to the engine working conditions. For this purpose, the flow characteristic of each injector, which gives the injected mass of water for a particular injection pressure as a function of the excitation time, must be obtained.

The injector is activated and controlled by the ADwin Gold-II control unit by means of a pulsed voltage signal. This signal is sent to a LM1949 injector driver controller. At high level, the driver lets current pass through the solenoid of the injector and the injector needle opens. At low level (0 V), the current through the injector will be cut off and the needle closes. In this way, the injection instant and the injection duration over the engine cycle can be easily controlled.

2.2. Engine test bed

The used CHP unit is a SenerTec Dachs G 5.5. It is driven by a naturally aspirated 4-stroke single-cylinder engine running on natural gas. The main characteristics and configuration of the engine used at the tests are listed in Table 2 and the CHP unit is shown in figure 4. For the experiments, the gas mass flow was regulated using a Maxitrol EXA Star modulating valve coupled to the gas multibloc. Trials were run with a modified piston to increase the compression ratio from 13.2:1 to 15.25:1.

Table 2. Engine specifications.

Engine type	SenerTec Dachs G 5.5 / swirl port
Nominal speed	2450 rpm
Compression ratio	15.25:1
Stroke	91 mm
Bore	90 mm
Displacement volume	580 ccm
Number of valves	2
Ignition system	prechamber spark plug

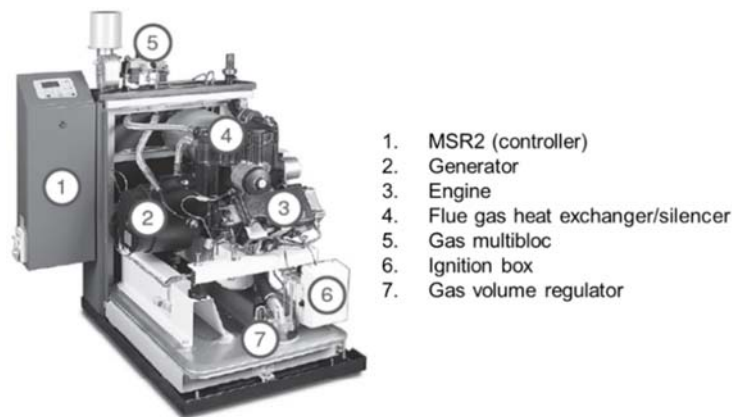


Figure 4. Dachs G 5.5 CHP unit [18].

Since water was to be injected before the intake valve of the engine, a special adapter was designed and coupled to the intake manifold as shown in figure 5a and figure 5b. Further, a thermocouple was mounted into the intake manifold and bent in order to measure gas temperature right before the intake valve in order to examine the effect of water injection on mixture cooling. The inclination angle of the injector was 45° with respect to the intake flow axis.

The water supply to the injector was made using flexible PTFE pipes, which resist the temperature of the engine housing and coupled to a connection situated at the upper part of the adapter.

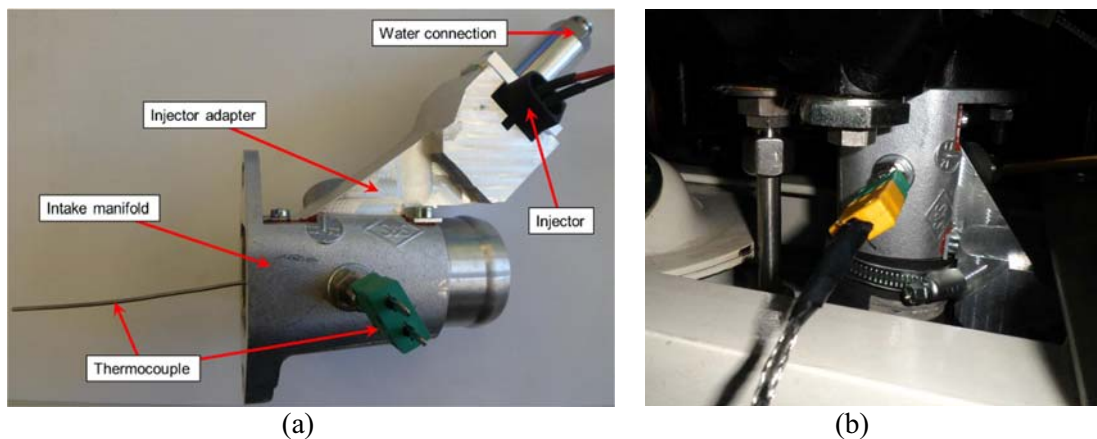


Figure 5. Injector adapter coupled to the intake manifold and thermocouple to measure the temperature near the intake valve (a), installation of the adapter at the gas engine (b).

A proprietary LabVIEW graphic user interface was employed to communicate with an ADwin Pro-II system responsible for controlling all engine actuators and slow data acquisition. Pressure at the different measuring points of engine were obtained using SITRANS P200 pressure sensors; the air mass flow was measured with a HFM5-4.7 hot film air flow meter calibrated for low-range mass flows; fuel mass flow was determined using a Bronkhorst F-103-low- Δp gas flow meter; λ was measured using a Bosch LSU 4.9 wideband lambda sensor. K-Type thermocouples were used to measure temperatures, connected to PICO TC-08 data loggers. A DEWE-800-CA combustion analyser was used for recording the in-cylinder pressure against crank angle and calculating combustion parameters.

Constant ambient conditions in terms of pressure and temperature at the air intake of the CHP unit were supplied using the same air conditioning unit as for the spray test bed.

Exhaust gas analysis was made using an ABB 6-component exhaust gas analyser with heated sample lines. A Multi FID 14 unit with a flame ionisation detector was used to measure wet total

hydrocarbons (THC). A Limas11 HW unit with a photometer after the DUV-RAS/NDUV (Differential Ultra Violet Resonance Absorption Spectroscopy / Non Dispersive Ultra Violet) principle was used to measure wet NO and NO₂ concentration. Dry CO₂ and CO were measured with an Uras14 unit equipped with an IR photometer. Dry O₂ concentration was measured using a Magnos 206 based on the paramagnetic properties of O₂.

3. Results and discussion

3.1. Injectors flow characteristics

The flow characteristics were obtained for the three injectors presented. They must be obtained to determine the relation between injector activation time and the water mass provided by the injector. Injector excitation time was set as described in section 2.1 and water was injected into a vessel, positioned on a Kern PLJ 6200-2AM precision balance. An average value over 3000 injection events was taken for each injector activation time. The maximum tank pressure that can be provided by the compressed air system and the given pressure reducer is 9 bar (absolute). Since the pressure regulation of the pressure reducer was slightly unstable at maximum pressure, the tested pressure level for the Denso and Bosch injector was reduced to 8.5 bar. For the Siemens injector, a pressure level of 4 bar was tested. Figure 6 shows the mass of water injected per injection event and the calculated equivalent water-fuel ratio.

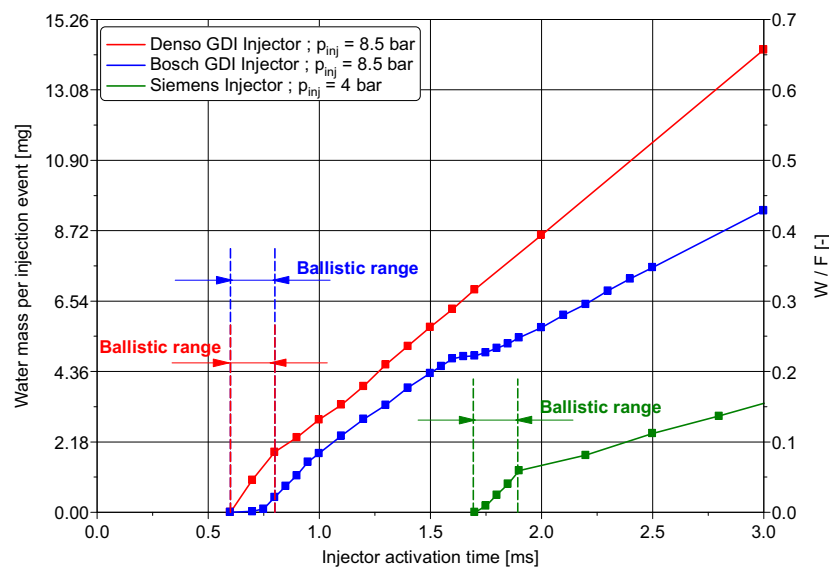


Figure 6. Flow characteristics of the three tested injectors.

As shown in the figure 6, the injector activation time, represented in x-axis, is not the same as the injector opening time. The injector needs a particular time to start opening, which is approximately 0.6 ms for the Denso and Bosch injectors, and 1.2 ms for the Siemens injector. Moreover, the injector needs a minimum opening duration to open the needle completely. This is known as the “ballistic” range of the injector and must be avoided for water injection operation. During this time, the water mass flow shows high cyclic fluctuations due to different needle lifts from cycle to cycle. Above the ballistic range, the injector shows a stable injection behaviour.

When comparing all injectors, it can be confirmed that the Siemens injector has a considerably lower water mass flow rate. The ballistic range for the three injectors is similar. The operating point of $W/F = 0.05$ is inside the ballistic range for all three injectors. For this reason, the lowest W/F ratio tested was set to 0.1. The Bosch injector has a lower mass flow rate as the Denso injector for the same ballistic range, allowing the injector to operate farther away from the ballistic range at $W/F = 0.1$, which can be taken as an advantage.

3.2. Tests at spray test bed

To study the spray propagation, images were taken at the spray test bed. For the GDI injectors, several injection pressure levels were tested. It was found that the angle of the cone was wider and the atomisation better as the pressures increased. Therefore, it was decided to operate the GDI injectors at the maximal possible injection pressure (8.5 bar). Figure 7 shows the images of the three sprays injected in an air mass flow of 40.8 kg/h, what corresponds approximately to the reading of the mean air mass flow of the engine at the series operating point. A binarization process of the images using Matlab was applied to further increase the contrast of the spray outline and the droplets.

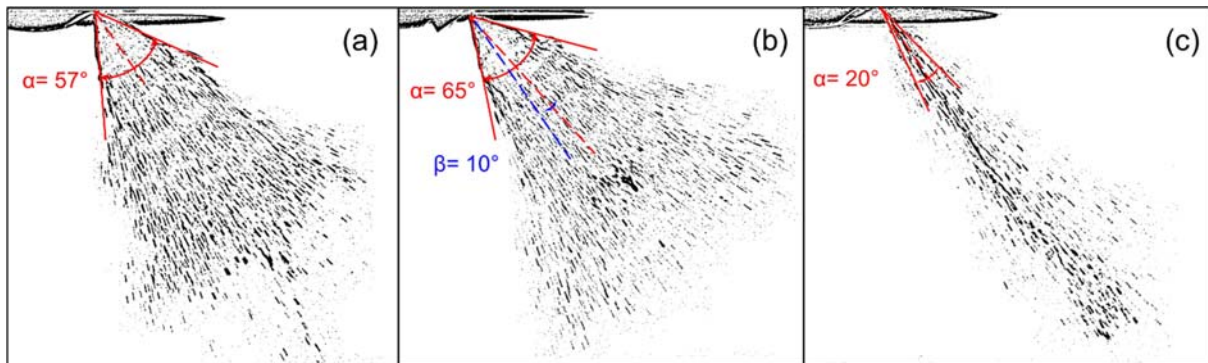


Figure 7. Water spray for Denso injector (a) and Bosch injector (b) after 3 ms injector excitation time; for Siemens injector (c) after 4.5 ms injector excitation time.

As can be seen from the images, the Siemens PFI injector has a smaller spray angle compared to the GDI injectors tested. This can cause a worsened dispersion of water, due to the lower volume of air mass flow covered by the spray. From the two swirl injectors, the Bosch injector has a larger cone angle and an inclination of the spray of $\beta = 10^\circ$ with respect to the injector axis, which allows orienting the spray more parallel to the air mass flow. These two factors improve the entrainment of droplets, reducing wall wetting compared to the Denso injector. Moreover, the Bosch injector achieves a slightly better atomisation.

In due consideration of the spray test findings and having to operate it farther away from the ballistic range, the Bosch injector was chosen for conducting the experimental trials presented in the following section.

3.3. Experimental Results

Engine trials were carried out at a constant IMEP of 6.35 bar. Intake air was conditioned at a constant intake pressure of 995 mbar and a constant temperature of 35 °C. The tested water-fuel ratios during the experiments were 0, 0.1, 0.2 and 0.3.

For each water-fuel ratio series, combustion phasing (CA50, defined as 50 % fuel mass fraction burnt) was varied by adjusting spark timing and λ . Each operating point was measured three times and the average value calculated. Combustion parameters were averaged over 200 engine cycles.

Figure 8a shows NO_x emissions against CA50) for each water-fuel ratio. NO_x emissions are expressed as specific emission output referenced g/kWh to indicated engine power. As it can be observed, NO_x emissions decrease for a constant CA50 when the injected water mass flow increases, due to the increase of the heat capacity of the mixture and the reduction of the combustion temperature. The absolute decrease of NO_x emissions is greater for advanced CA50. The relative decrease for $W/F = 0.3$ compared to $W/F = 0$ varies between 20 % and 25 %, depending on combustion phasing.

Figure 8b shows the NO_x -ISFC trade-off for different water-fuel ratios. In the low NO_x regime of the diagram and at constant NO_x , water injection allows decreasing ISFC. For a constant ISFC of 204.1 g/kWh_i, which approximately matches with series combustion phasing (CA50 = 19°CA ATDC), the reduction in NO_x for $W/F = 0.3$ is approximately 0.2 g/kWh_i (15 %).

On the contrary, in the high efficiency regime region of the diagram, increasing fractions of water appear to be detrimental to ISFC.

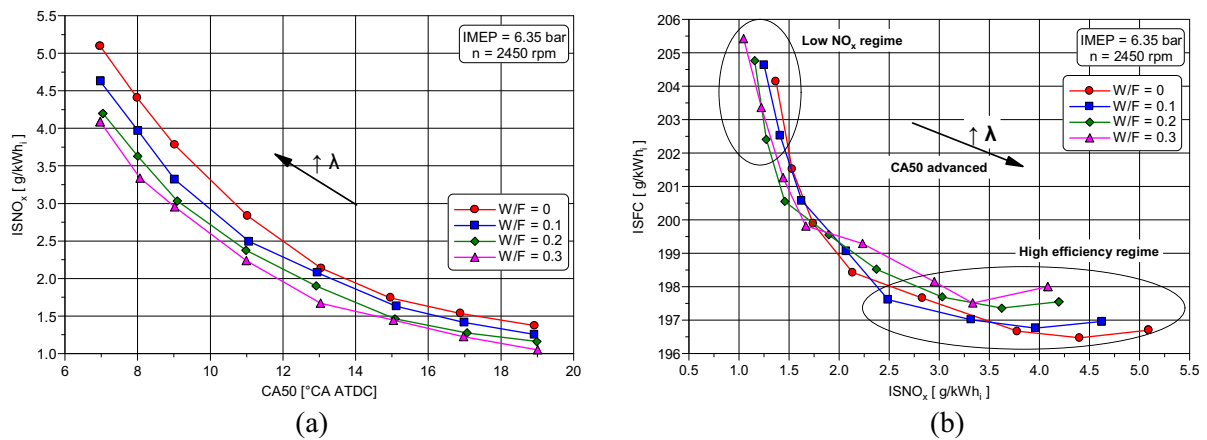


Figure 8. NO_x emissions against combustion phasing CA50 and water-fuel ratio (a), ISNO_x-ISFC trade-off for different water-fuel ratios (b).

Figure 9 shows NO_x emissions calculated according the 2018 new European normative. It can be seen that even a water-fuel ratio of 0.3 is not yet sufficient to meet the new limit.

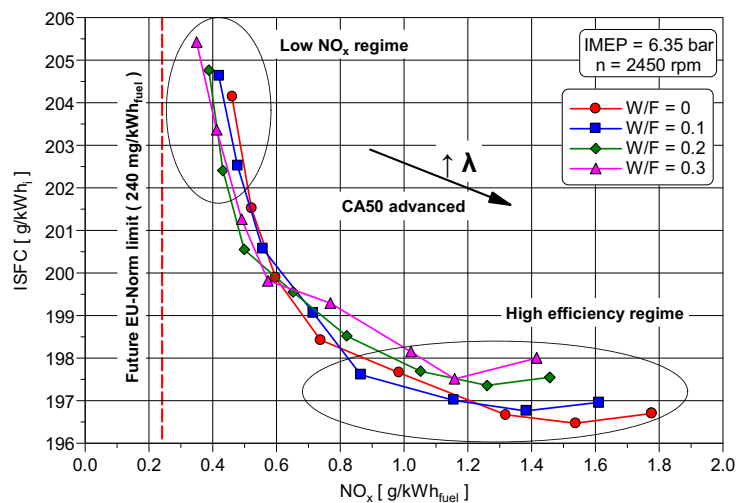


Figure 9. NO_x-ISFC trade-off calculated according to new 2018 EU normative.

Figure 10 shows the dependence of mixture temperature at the intake valve on the water-fuel ratio. Mixture temperature is fairly constant for each water-fuel ratio series and shows no dependence on combustion parameters. For W/F = 0.3 a cooling of the mixture at the intake valve of approximately 24 K is achieved.

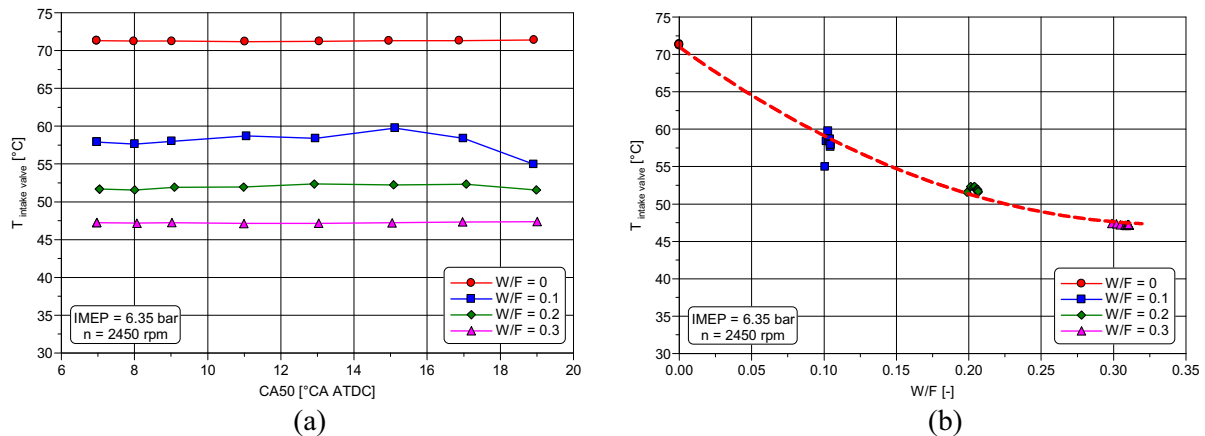


Figure 10. Mixture temperature at the intake valve depending as a function of CA50 (a) and the water-fuel ratio (b).

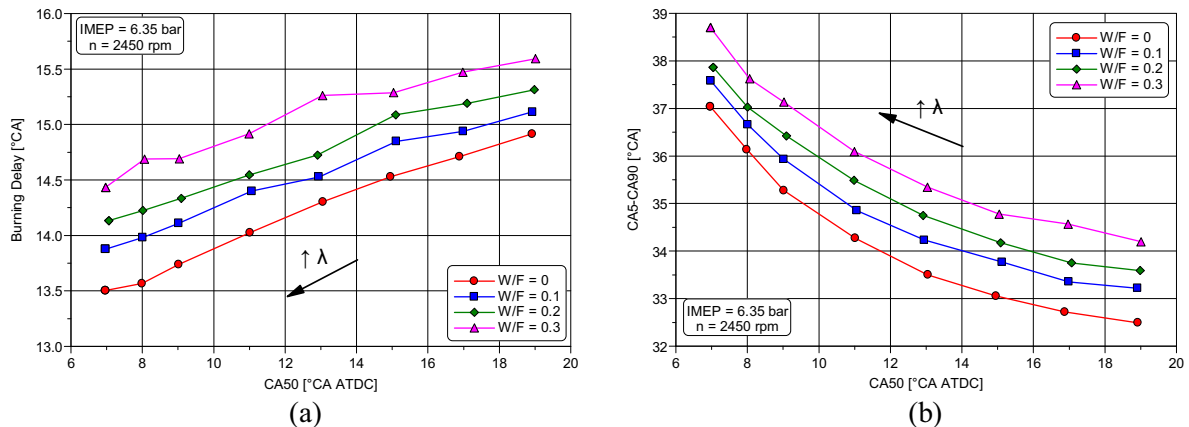


Figure 11. Burning delay (a) and combustion duration (b) as a function of combustion phasing CA50.

According to Halter et al. [7], the dilution of an air-fuel mixture with nitrogen and carbon dioxide causes a decrease of the laminar burning velocity, which leads to a slower combustion. In the same way, the addition of EGR (with the main constituents H_2O , CO_2 , N_2 and O_2) to the intake mixture implies a decrement of the burning velocity, as determined by Neher et al. [16] for different dilution ratios. For water injection, a higher dilution of the charge also increases the burning delay periods and the combustion duration, as it was exposed by several authors [8][13][23]. Figure 11a and figure 11b show that both burning delay and combustion duration increase with water injection. Burning delay is defined as the time in °CA between spark timing and the start of combustion. CA5 is taken as start of combustion and it is defined as 5 % mass fraction burnt. Combustion duration is defined as the time in CA between start of combustion (CA5) and end of combustion (CA90, defined as 90 % mass fraction burnt). As expected, burning delay and the duration of the combustion are affected by water injection and the tendency agrees well with the data found in the previously mentioned research work.

HC and CO emissions are presented in figure 12. As it can be observed, water injection enhances the formation of HC. This is caused by the lower combustion velocity, which leads to incomplete combustion phenomena. The same effect can be found for a constant W/F. When λ increases, the fraction of air in the mixture increases; it is more diluted and leads to incomplete combustion and a rise of HC emissions [10]. A clear tendency of CO emissions with injected water mass flow (figure 12b) cannot be found. For a constant W/F, the CO emissions increase when λ increases, because the reactions of CO formation are favoured by the presence of O_2 [15].

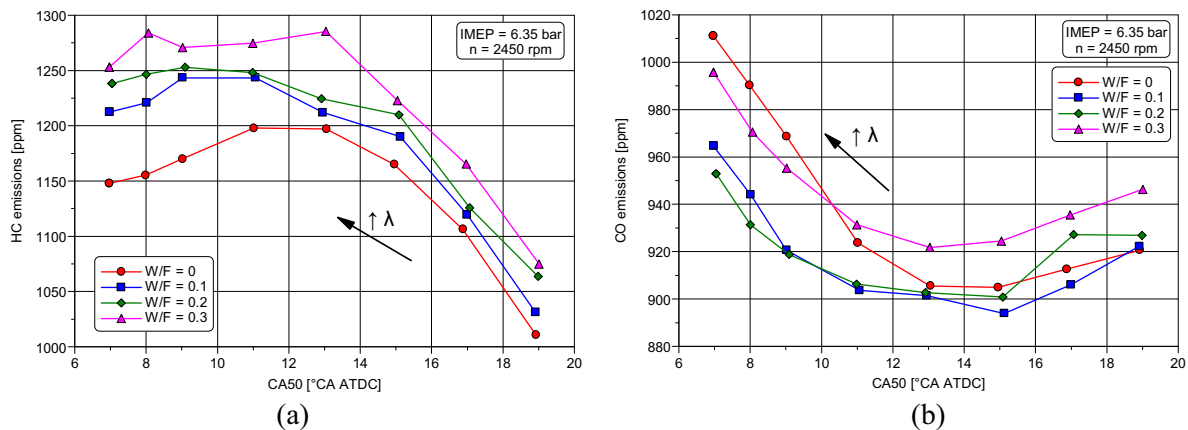


Figure 12. HC emissions (a) and CO emissions (b) depending on the water-fuel ratio.

Figure 13 depicts the coefficient of variance of IMEP. It is defined as the standard deviation of the IMEP divided by the mean value of IMEP, calculated from the ensemble of 200 cycles recorded. Engine stability and combustion variability normally deteriorates when the mixture becomes more dilute, as it occurs when leaning or by addition of EGR [10]. In a similar way, charge dilution by water injection, increases combustion instability, as it can be deduced from figure 13. However, the increase in COV is marginal and the obtained instability levels are acceptable. Much larger fractions of water could be injected until the stability of the combustion would be significantly affected.

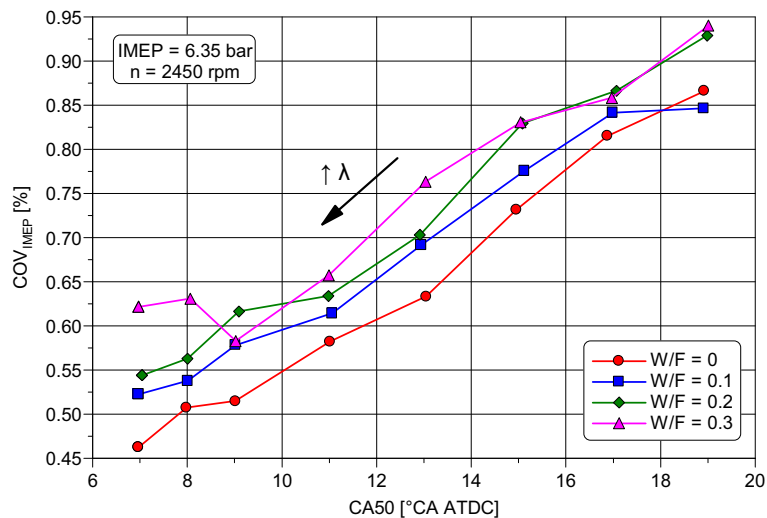


Figure 13. Calculated COV_{IMEP} of the combustion depending on the CA50.

4. Conclusions

In the present work, a system of intake manifold water injection for a small natural gas spark ignited engine was developed and tested. A Bosch swirl injector was selected in a spray test bed due to the better atomization, the better orientation of the spray and the most appropriate water mass flow of the injector for the engine operating conditions.

Subsequently, the selected injector was tested on the engine test bed. During the experiments, IMEP was kept constant at 6.35 bar. The following findings were obtained:

- In the low NO_x regime (late combustion phasing) at a constant ISFC of about 204 g/kWh_i, a reduction of ISNO_x of approximately 0.2 g/kWh_i (15 %) at W/F = 0.3 was achieved.
- For high efficiency regime (advanced combustion phasing), increasing the injected water mass causes a higher ISFC for constant NO_x.

- The evaporation enthalpy of the injected water allows decreasing intake mixture temperature by 24 K at W/F = 0.3.
- Increasing the water-fuel ratio increases burning delay, combustion duration and combustion instability.
- Injecting water increases HC emissions, while a tendency for CO emissions could not be found.

Intake manifold water injection has shown potential to reduce the NO_x output of the engine without losses in engine efficiency. Future research will focus on increasing the water-fuel ratio for further reductions in NO_x and analysing the potential of water injection for different compression ratios.

Acknowledgments

The authors would like to thank the German Federal Ministry of Education and Research, which supported this project through the grant programme “IngenieurNachwuchs”, as well as all persons that were involved in the project.

References

- [1] Ashgriz N 2011 Handbook of Atomization and Sprays. Theory and Applications (Springer)
- [2] Backhaus R Gemischbildung und Verbrennung 2016 *Motortechnische Zeitschrift* **77(4)** 14-15
- [3] Böhm M, Mährle W, Bartelt C and Rubbert S Funktionale Integration einer Wassereinspritzung in den Ottomotor 2016 *Motortechnische Zeitschrift* **77(1)** 38-43
- [4] Bosch GmbH H₂O statt CO₂. Wassereinspritzung für Benzinmotoren URL: <http://www.bosch-waterboost.de>
- [5] Bozza F, De Bellis V and Teodosio L Potentials of cooled EGR and water injection for knock resistance and fuel consumption improvements of gasoline engines 2016 *Applied Energy* **169** 112-125
- [6] European Commission Ecodesign requirements for space heaters and combination heaters, Regulation Nr. 813/2013 for execution of Norm 2009/125/EG
- [7] Halter F, Foucher F, Landry L and Mounaim-Rousselle Effect of Dilution by Nitrogen and/or Carbon Dioxide on Methane and Iso-Octane Air Flames 2009 *Combustion Science and Technology* **181** 813-827
- [8] Harrington J A Water Addition to Gasoline-Effect on Combustion, Emissions, Performance, and Knock 1982 *SAE Technical Paper* 820314
- [9] Herdin G Skriptum Grundlagen Gasmotoren 2012
- [10] Heywood J B 1988 *Internal combustion engine fundamentals* (McGraw-Hill)
- [11] Hoppe F, Thewes M, Baumgarten H and Dohmen J Water injection for gasoline engines: Potentials, challenges, and solutions 2016 *International Journal of Engine Research* **17** 86-96
- [12] Kettner M, Dechent S, Hofmann M, Huber E, Arruga H, Mamat R and Najafi G Investigating the influence of water injection on the emissions of a diesel engine 2016 *Journal of Mechanical Engineering and Sciences* **10(1)** 1863-1881
- [13] Kim J, Park H, Bae C, Choi M and Kwak Y Effects of water direct injection on the torque enhancement and fuel consumption reduction of a gasoline engine under high-load conditions 2016 *International Journal of Engine Research* **17(7)** 795-808
- [14] Kökkülünk G, Gonca G, Ayhan V, Cesur I and Parlak A Theoretical and experimental investigation of diesel engine with steam injection system on performance and emission parameters 2013 *Applied Thermal Engineering* **54** 161-170
- [15] Merker G P, Schwarz C and Teichmann R 2012 *Combustion Engines Development. Mixture Formation, Combustion, Emissions and Simulation* (Springer)
- [16] Neher D, Scholl F, Kettner M, Schwarz D, Klaisle M and Giménez Olavarría B The Effect of Cooled Exhaust Gas Recirculation for a Naturally Aspirated Stationary Gas Engine 2016 *SAE International Journal of Engines* **9(4)** 2477-2492

- [17] Pucher H and Netzel H NO_x-Senkung bei Gasmotoren durch Saugrohr-Wassereinspritzung 1984 *Motortechnische Zeitschrift* **45(1)** 33-35
- [18] SenerTec Kraft-Wärme-Energiesysteme GmbH
- [19] Subramanian V, Mallikarjuna J M and Ramesh A Effect of water injection and spark timing on the nitric oxide emission and combustion parameters of a hydrogen fuelled spark ignition engine 2007 *International Journal of Hydrogen Energy* **32** 1159-1173
- [20] Thewes M, Hoppe F, Baumgarten H and Seibel J Wassereinspritzung für ottomotorische Brennverfahren 2015 *Motortechnische Zeitschrift* **76(2)** 26-31
- [21] Tschalamoff T, Laaß U and Janicke D Direkte Wassereinspritzung im mittelschnelllaufenden Gasmotor 2007 *Motortechnische Zeitschrift* **68(11)** 954-962
- [22] Tschalamoff T and Sahl C Saugrohr-Wassereinspritzung an einem Ottogasmotor 2009 *Proceedings of 6th Dessau Gas Engine Conference* 186-196
- [23] Wei M, Nguyen T S, Turkson R F, Guo G and Liu J The Effect of Water Injection on the Control of In-Cylinder Pressure and Enhanced Power Output in a Four-Stroke Spark-Ignition Engine 2016 *Sustainability* **8(10)** 993